

Stream-discharge surges generated by groundwater flow

Adrien Guérin¹, Olivier Devauchelle¹, Vincent Robert¹, Thierry Kitou¹, Céline Dessert¹, Amélie Quiquerez², Pascal Allemand³, and Eric Lajeunesse¹

¹Institut de Physique du Globe de Paris, Sorbonne Paris Cité, Université Paris Diderot, UMR 7154 CNRS,
1 rue Jussieu, 75238 Paris, Cedex 05, France

²Université de Bourgogne, UMR CNRS 6298, ARTeHIS, 6 Boulevard Gabriel, 21000 Dijon, France

³Université Claude Bernard Lyon 1, Ens de Lyon, CNRS, UMR 5276 LGL-TPE, F-69622, Villeurbanne,
France

Key Points:

- High-frequency measurements show that groundwater non-linearly amplifies the response of a catchment to rainfall events.
- The storm-flow regime of the underground flow consistently predicts the peak runoff.
- We propose a method to measure the available volume of groundwater stored in a shallow aquifer based on its catchment's hydrograph.

Corresponding author: Olivier Devauchelle, devauchelle@ipgp.fr

Abstract

Catchments respond to rainfall by storing and releasing water according to their internal dynamics. Groundwater had long been treated as the slow reservoir in this process, but isotopic measurements showed how responsive it can be. Here, we investigate the mechanics of groundwater's contribution to floods. To do so, we monitored over three years the shape of the water table in, and the runoff out of, a small tropical catchment. We find that groundwater and runoff respond within minutes of a rainfall event. Using an asymptotic theory inspired by recent laboratory experiments, we suggest that the peak water discharge at the catchment's outlet increases like the rainfall rate to the power of $3/2$. This formula consistently predicts the stream's response to the 137 isolated rainfall events recorded during our field survey. In addition, its prefactor yields an estimate of the average groundwater storage.

Plain Language Summary Rainwater infiltrates into the ground, accumulates in porous rocks, and eventually flows towards a neighboring stream. Although this underground travel often takes millennia, groundwater can contribute quickly to floods. To understand how an underground flow can be so responsive, we have recorded the motion of the groundwater surface in a small tropical catchment during three years. We find that groundwater swells within minutes of a rain event, and that this deformation directly pushes more water into the stream. The resulting stream-discharge peak strengthens faster than the rainfall intensity: a three-fold increase of the latter causes a five-fold increase of the stream discharge. Including this mechanism into flood-forecasting models should allow us to better predict the impact of extreme precipitations. Finally, we introduce a method to measure how much water an aquifer stores during a rainfall event, before releasing it—a central parameter for the management of water resources.

1 Introduction

The typical hydrograph of a river draining a small catchment (i.e. the time series of its discharge) increases steeply during rainfall, and declines slowly afterward, as groundwater reservoirs empty into the drainage system (Sefton, Whitehead, Eatherall, Littlewood, & Jakeman, 1995). Catchments thus shape their response to rainfall by storing water, and then releasing it into the network of streams that drains them (Harman & Sivapalan, 2009; Kirchner, 2009). Understanding this process is a formidable task: before it reaches a stream, rainwater infiltrates into the vadose zone (Maher, DePaolo, Conrad, & Serne, 2003), is absorbed by the roots of trees (Mares, Barnard, Mao, Revil, & Singha, 2016), and eventually joins the groundwater zone, where it flows through heterogeneous and fractured rocks (Berkowitz, 2002; De Marsily et al., 2005; Goderniaux, Davy, Bresciani, Dreuzy, & Le Borgne, 2013). There is little doubt that it is groundwater that sustains the recession limb of a hydrograph after a rainfall event (Brutsaert & Nieber, 1977). During the event itself, however, the significance of its contribution to the rising limb of the hydrograph remains debated (Kirchner, 2003). Most streams remain chemically close to groundwater even at their peak discharge, indicating that groundwater can respond quickly to rainfall (Jasechko, Kirchner, Welker, & McDonnell, 2016; McDonnell, 2003; Neal & Rosier, 1990; M. Sklash, 1990). For this to happen, the vadose zone must promptly transmit the rainfall signal to the water table, but the mechanisms by which it does so remain controversial (McDonnell et al., 2010). Likely candidates include water flowing through non-capillary cracks (Beven & Germann, 1982; McDonnell, 1990; McGlynn, McDonnell, & Brammer, 2002; Tromp-van Meerveld & McDonnell, 2006), and ridging in the capillary fringe (Abdul & Gillham, 1984; Cloke, Anderson, McDonnell, & Renaud, 2006; Fiori, Romanelli, Cavalli, & Russo, 2007; M. G. Sklash & Farvolden, 1979).

Once it reaches the water table, rainwater raises the pressure in the groundwater zone. How the water table responds to this change in the pressure field, and ultimately pushes

66 water into the drainage network, depends on the aquifer’s geometry. In steep and shallow
 67 aquifers, the rainfall signal travels as a kinematic wave driven by gravity (Beven, 1981;
 68 Tani, 1997). In more typical aquifers, however, it is the pressure gradient that drives the
 69 flow through the porous rock. In general, one then needs to consider both the horizontal
 70 and vertical components of the groundwater flow which, in steady state, determine the flow
 71 pattern and the distribution of the transit time through the aquifer (Cardenas, 2007; Toth,
 72 1963). Dynamical simulations in unconfined aquifers prove more challenging.

73 When permeability decreases steeply with depth, or when an impervious horizon
 74 bounds the groundwater flow, the latter is mostly horizontal, and one can combine Darcy’s
 75 law to the shallow-water approximation to derive the Boussinesq equation (Boussinesq, 1904;
 76 Dupuit, 1848). Brutsaert and Nieber (1977) used this equation, in its original non-linear
 77 form, to estimate the hydraulic properties of an unconfined aquifer based on the recession
 78 limb of its hydrograph. This method, and the associated power-law of the recession limb,
 79 has since become a staple of groundwater hydrology (Troch et al., 2013, and references
 80 therein).

81 Only recently, however, has the Boussinesq equation been invoked to represent the
 82 rising limb of a hydrograph (Pauwels & Troch, 2010). Based on numerical solutions of
 83 the linearized Boussinesq equation, Fiori (2012) showed that it could simulate a complete
 84 hydrograph, and explain the chemical composition of the groundwater that feeds a stream
 85 during a rainfall event. Pauwels and Uijlenhoet (2019) confirmed the validity of this equation
 86 in gently sloping laboratory aquifers submitted to a sudden rainfall event, showing that
 87 unconfined aquifers react virtually instantly to a rainfall input. These results, however,
 88 must be reconciled with the power-law recession of the hydrograph, which can result only
 89 from the non-linear Boussinesq equation. Laboratory experiments achieve this reconciliation
 90 when the aquifer’s outlet, which represents a stream, coincides with the impermeable base
 91 of the aquifer (Guérin, Devauchelle, & Lajeunesse, 2014). In this configuration, the flow
 92 can enter a new asymptotic regime (the “storm-flow regime”), during which the aquifer’s
 93 discharge increases in proportion to $R_s^{3/2}$, where R_s is the recharge rate.

94 If it occurs in nature, this non-linear regime would especially amplify the most intense
 95 rainfall events. To our knowledge, however, it has never been identified in the field. Here,
 96 we combine high-frequency field measurements with the classical Boussinesq approximation
 97 to seek out the storm-flow regime in a small catchment.

98 2 Field Setup

99 To identify the storm-flow regime in a natural setting, we instrumented an eight-
 100 hectare catchment in the volcanic island of Basse-Terre, in the Guadeloupe archipelago,
 101 French West Indies (Figure 1a). There, the pristine forest of the Guadeloupe National Park
 102 covers an at least 10 m-thick layer of unconsolidated clay (Buss et al., 2010; Clergue et al.,
 103 2015) (Figure 1b), the hydraulic conductivity of which typically ranges from about 10^{-6}
 104 to 10^{-5} m s^{-1} depending on compaction and composition (Colmet-Daage & Lagache, 1965,
 105 Supporting Information Text S1). An electrical resistivity tomography survey revealed a
 106 homogeneous aquifer, with no visible horizon in the clay layer (Supporting Information
 107 Text S1 and Figure S1). This shallow catchment (its surface slope is 14° on average) is
 108 drained by the Quiocq creek, a stream less than 2 m wide. Outside this stream and its
 109 tributaries, the catchment shows no indication of surface runoff—the ground is permanently
 110 littered with decaying leaves.

111 Modern pressure transducers can record high-frequency measurements over months
 112 without human intervention, making it possible to monitor accurately the response of
 113 groundwater to a long series of rainfall events. We installed eight such transducers in
 114 the Quiocq catchment, seven of which in piezometric wells arranged in a linear array which
 115 extends, perpendicularly to the stream, over 30 m (Figure 1c). This disposition allows us to

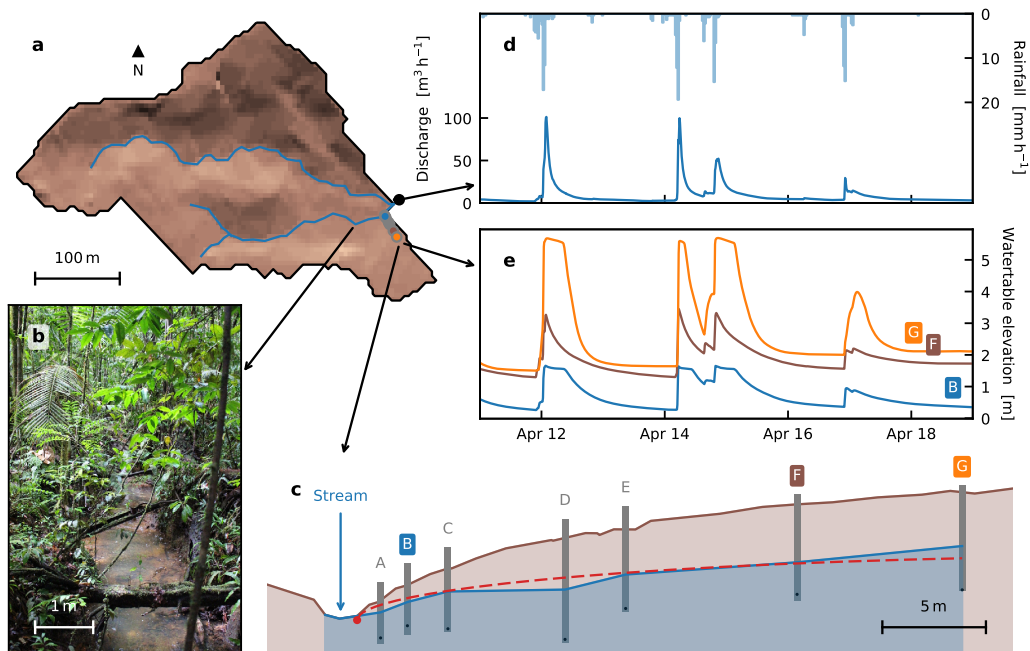


Figure 1. Instrumented catchment of the Quiock creek, Guadeloupe, French West Indies. (a) Map of the catchment ($16^{\circ} 10' 36''$ N, $61^{\circ} 41' 44''$ W). Dots indicate piezometric wells. (b) Quiock creek about 10 m upstream of measurements. (c) Cross section of the shallow aquifer. Blue line shows the root mean square of the water table profile, h_{RMS} , from January 2015 to October 2017. Red dashed line corresponds to equation (1). Brown shaded area, grey lines and black dots indicate ground surface, boreholes and pressure sensors respectively. (d) Time series of the stream discharge and rainfall rate (April 2015). (e) Time series of the water-table elevation, with respect to stream level, at 2.4, 21 and 29 m from the river.

116 reconstruct the shape of the groundwater surface every minute. We placed the eighth trans-
 117 ducer in a stream gauge to record the discharge of the Quiock creek at the same frequency.
 118 In addition, a tipping-bucket rain gauge measures precipitations less than 10 m away from
 119 the wells, below the canopy (Supporting Information Text S2).

120 3 Observations

121 We find that the Quiock catchment, like most catchments of its size, distorts the rain
 122 signal (Figure 1d). Right after the beginning of a rain event, the runoff increases quickly,
 123 sometimes tenfold within a few minutes. After the rain has stopped, the stream's discharge
 124 begins a recession that lasts until the next event, often days later.

125 Remarkably, although the groundwater surface lies a few meters below ground, it rises
 126 virtually instantly (Figure 1e), so much so that our measurements cannot tell which, of the
 127 groundwater or the stream, reacts first (Supporting Information Text S4 and Figure S2).
 128 This observation indicates that the pressure jump induced by fresh rainwater propagates
 129 through the vadose zone at a velocity of a few millimeters per second at least, before the
 130 water table responds to it. This fast transfer of the rainfall signal, common to many catch-
 131 ments (Abdul & Gillham, 1989; Sidle et al., 2000; Tromp-van Meerveld & McDonnell, 2006),
 132 remains the subject of active research (Cloke et al., 2006).

133 To interpret our observations, we first need to estimate the geometry and hydrological
 134 properties of the aquifer. We represent the former as simply as possible, by assuming that the
 135 groundwater flow is mostly orthogonal to the river. Accordingly, we estimate its horizontal
 136 extension L_a as half the average distance between two rivers, namely $L_a = A/(2L_r)$, where
 137 A is the area of the catchment, and L_r the total length of its drainage network. Based on
 138 the Lidar map of Figure 1a, we find $L_a \approx 40$ m.

139 We further assume (i) that there exists, at the catchment scale, a representative hy-
 140 draulic conductivity K (Sanchez-Vila, Guadagnini, & Carrera, 2006), and (ii) that most of
 141 the groundwater flows horizontally in an active layer, above the stream elevation. If correct,
 142 these assumptions open the toolbox of the Boussinesq approximation: the pressure head
 143 in the aquifer is hydrostatic, and the Darcy flow it drives is induced by the local elevation
 144 of the water table (Boussinesq, 1904; Brutsaert & Nieber, 1977; Dupuit, 1848). Strictly
 145 speaking, approximation (ii) (often referred to as the “fully-penetrating stream”) holds only
 146 when an impervious horizon joins the stream, and confines the groundwater flow above it-
 147 self. We have no indication that such is the case in the Quiock catchment. One often finds,
 148 however, that the hydraulic conductivity of unconsolidated aquifers quickly decreases with
 149 depth, possibly due to compaction (McKay, Driese, Smith, & Vepraskas, 2005; Montgomery
 150 et al., 1997; Schoeneberger & Amoozegar, 1990). We expect that such a vertical gradient
 151 of conductivity would confine most of the flow to the layers lying above the stream. We
 152 cannot assess the validity of this point a priori; instead, we will deem it plausible as long as
 153 the catchment’s behavior accords with it (Harman & Sivapalan, 2009). Asymptotic regimes,
 154 in particular, are sensitive to the physical mechanism that drives them (Barenblatt, 1996),
 155 and those of the Boussinesq equation would break down if the shallow-flow approximation
 156 were grossly inadequate. In the following, we interpret two of them as the signature of a
 157 shallow flow.

158 Averaging the Boussinesq equation over a sufficiently long period yields the textbook
 159 expression for the shape of a steady water table (Supporting Information Text S5):

$$h_{\text{RMS}} = \sqrt{\frac{\langle R \rangle}{K} x (2L_a - x)} \quad (1)$$

160 where x is the distance to the stream, $\langle R \rangle$ is the average recharge rate and $h_{\text{RMS}} = \sqrt{\langle h^2 \rangle}$ is
 161 the root mean square of the water table elevation. That h_{RMS} appears in the above equation,
 162 as opposed to the average elevation of the water table $\langle h \rangle$, results from the non-linearity of
 163 the Boussinesq equation (Eq. (2), Supporting Information Text S5). Here, we define h_{RMS}
 164 with respect to the stream’s elevation, in accord with approximation (ii). Fitting the ratio
 165 $\langle R \rangle/K$ to our observations (Figure 1c), and estimating the recharge rate as the ratio of the
 166 average stream discharge to the area of the catchment, we find a catchment-scale hydraulic
 167 conductivity of $K = 5.6 \times 10^{-6} \text{ m s}^{-1}$, within the range of expected values for unconsolidated
 168 clay (Supporting Information Text S5).

169 Integrating h_{RMS} over the entire catchment yields an estimate of the aquifer volume
 170 that, on average, holds water above the stream’s level :

$$V_r = \frac{\pi A L_a}{4} \sqrt{\frac{\langle R \rangle}{K}} \approx 1.9 \times 10^5 \text{ m}^3 . \quad (2)$$

171 This volume occupies a significant part of the available space in the aquifer, between the
 172 stream’s level and the ground surface (Figure 1c). When rainfall reaches the water table,
 173 the aquifer’s matrix gets refilled with water, in proportion to its fillable porosity ϕ_f —the
 174 ratio of the pore volume available to the rising water table to the total volume (Acharya,
 175 Jawitz, & Mylavarapu, 2012; Park & Parker, 2008; Sophocleous, 1991). Multiplying V_r with
 176 the fillable porosity thus yields an estimate of the volume of water, $V_a = \phi_f V_r$, that the
 177 aquifer stores above the stream’s level, on average. In the framework of the Boussinesq
 178 approximation, this is the total volume of groundwater that, on average, would be released
 179 into the stream during a prolonged drought; we name it “available volume” on that account.

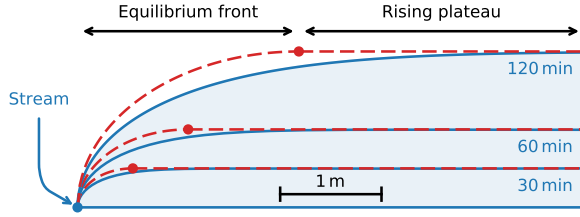


Figure 2. Theoretical shape of the water table during the storm-flow regime. For illustration, $R_s = 10 \text{ mm h}^{-1}$, $\phi_f = 1.3 \times 10^{-2}$ and $K = 5.6 \times 10^{-6} \text{ m s}^{-1}$. Blue lines: self-similar solution of the Boussinesq equation (Guérin et al., 2014). Red dashed lines: approximate self-similar solution. Red dots indicate the transition between the equilibrium front and the rising plateau, at $x = L_f$.

180 Dividing this volume by the average discharge of the catchment yields a characteristic time,
 181 $T_c = V_a / \langle Q \rangle$ which, at this point, is merely a mathematical definition. We will see, however,
 182 that it will prove a convenient parameter to represent the reaction of the groundwater flow
 183 to a rainfall event.

184 We now use the recession of the water table after a rain to evaluate the validity of
 185 the Boussinesq approximation in the Quiock catchment, and to characterize its shallow
 186 aquifer (Rupp, Schmidt, Woods, & Bidwell, 2009; Troch et al., 2013). Once rainfall has
 187 stopped, the water table decreases in all piezometric wells, although at different rates, as
 188 the aquifer drains slowly into the stream. Since we monitor simultaneously the stream
 189 discharge and the water table elevation, we may compare their evolution to the predictions
 190 of the Boussinesq approximation, and adjust the aquifer’s hydraulic properties to fit the
 191 theory to our observations. During a dry period, the water table should decrease as the
 192 inverse of time, while the discharge of the stream decreases as the squared inverse of time
 193 (Brutsaert & Nieber, 1977). The Quiock aquifer accords with this theory (Supporting
 194 Information Text S6 and Figure S3), and we find a drainable porosity of $\phi_d \approx 5.3 \times 10^{-2}$,
 195 an ordinary value for clay (Batu, 1998). This analysis also yields another estimate for the
 196 hydraulic conductivity, $K \approx 4.1 \times 10^{-6} \text{ m s}^{-1}$, which is consistent with the estimate based
 197 on equation (1). These findings supports the assumption, so far unsubstantiated, that the
 198 permeability of the aquifer decreases quickly below the stream’s level, and encourage us to
 199 use the non-linear Boussinesq equation during the early stage of a rainfall event as well. In
 200 the next section, we analyze our observations in search of the storm regime.

201 4 Storm-flow Regime

202 After a drought, the water table is low and the stream discharge recedes. The next
 203 rainfall event abruptly increases the groundwater pressure throughout the shallow aquifer,
 204 which responds by expelling more water into the neighboring stream. Following Guérin et
 205 al. (2014), we now idealize this scenario by considering an initially empty aquifer suddenly
 206 recharged at rate R_s . Under these assumptions, the groundwater flow enters the storm-flow
 207 regime of the Boussinesq equation, the mathematical expression of which was derived by
 208 Guérin et al. (2014) (Supporting Information Text S7). Here we propose a simpler derivation
 209 which better illuminates the mechanics of this peculiar regime, at the cost of mathematical
 210 rigour.

211 Figure 2 shows the theoretical shape of the water table as it swells to accommodate
 212 the rainfall input (Guérin et al., 2014). We now approximate this mathematical solution
 213 by splitting it into two connected regions. Far from the outlet, the water table rises at

214 velocity R_s/ϕ_f , unaffected by the groundwater lost to the stream. Meanwhile, a smooth
 215 front of length L_f connects the outlet to this rising plateau. Along this front, the water
 216 table is virtually at equilibrium with the recharge. Since, in this simple reasoning, the rising
 217 plateau delivers no water to the front, the groundwater discharge per unit length of stream
 218 is $R_s L_f$ —collected entirely by the front. The front’s shape is that of a steady water table
 219 in an aquifer of length L_f , that is, equation (1) in which we substitute $\langle R \rangle$ with R_s , and L_a
 220 with L_f . However, the front is not exactly at equilibrium, since it needs to match the height
 221 of the rising plateau; this requires that the front’s thickness increase linearly with time,
 222 according to $L_f = \sqrt{K R_s} t / \phi_f$, where t is the time elapsed since the beginning of recharge.
 223 This matching yields the approximate shape of the water table in the storm-flow regime
 224 (red lines in Figure 2). Although not rigorous, this procedure yields the same expression as
 225 Gu erin et al. (2014), but for a prefactor of order one.

226 Unfortunately, in the Quiock catchment, the spatial resolution of our water-table mea-
 227 surements does not allow for a direct comparison between the actual water table and the
 228 solution derived above. Indeed, after one hour of sustained and intense rainfall, we expect
 229 the equilibrium front to extend over a few meters only (Figure 2). Instead, we may calculate
 230 the amount of groundwater the aquifer delivers to the stream during a rainfall event, and
 231 compare it to the associated discharge surge we measure in the stream, ΔQ_s . To do so,
 232 we first derive the groundwater flow that exits the aquifer in the storm regime at time T_s
 233 (Supporting Information Text S7):

$$\Delta Q_s \approx 2L_r \frac{\sqrt{K}}{\phi_f} R_s^{3/2} T_s. \quad (3)$$

234 This expression is similar to the equation derived by Gu erin et al. (2014), but for a numerical
 235 prefactor of about 0.73, which is accessible only to a thorough mathematical derivation of
 236 the storm-flow regime. As expected, we recover the exponent of 3/2 that distinguishes the
 237 storm-flow regime. The above equation also shows that the storm flow, like most asymptotic
 238 regimes in dissipative systems, does not depend on initial conditions (i.e. the shape of the
 239 water table before the rainfall event). How decent an approximation this mathematical
 240 feature will prove in practice is, at this point, open to question.

241 Equation (3) involves parameters that are sometimes difficult to measure (L_r , K and
 242 ϕ_f), and the recharge rate raised to a non-integer exponent—a quantity whose dimensions
 243 are hardly meaningful. To produce a more presentable version of Eq. (3), we divide it by
 244 the average water balance for the catchment, namely $\langle Q \rangle = A \langle R \rangle$. We thus get

$$\frac{\Delta Q_s}{\langle Q \rangle} \approx \frac{2L_r \sqrt{K \langle R \rangle}}{A \phi_f} \left(\frac{R_s}{\langle R \rangle} \right)^{3/2} T_s. \quad (4)$$

245 Finally, using Eq. (2) to express the characteristic time T_c of the aquifer in terms of the
 246 hydraulic properties of the latter, we rewrite Eq. (4) as:

$$\frac{\Delta Q_s}{\langle Q \rangle} = C \frac{T_s}{T_c} \left(\frac{R_s}{\langle R \rangle} \right)^{3/2}, \quad (5)$$

247 where $C \approx 0.57$ is the numerical prefactor derived by Gu erin et al. (2014) (Supporting
 248 Information Text S7). The above equation is equivalent to Eq. (3), but perhaps more
 249 telling. Its advantages are that (i) all quantities are made non-dimensional using their
 250 average value, and (ii) the hydrological properties of the aquifer are all lumped into a
 251 single free parameter, the characteristic time T_c (or, equivalently, the available volume V_a).
 252 These advantages, however, come at a cost: the presence of average quantities ($\langle Q \rangle$, T_c and
 253 $\langle R \rangle$) in Eq. (5) might suggest that the prefactor of this power-law depends on the average
 254 hydrological conditions. In fact, however, a change in the average rainfall rate would affect
 255 $\langle Q \rangle$ and $T_c \langle R \rangle^{3/2}$ in the same proportion, and Eq. (5) would thus remain unaffected—so
 256 long as the groundwater flow has entered the storm-flow regime.

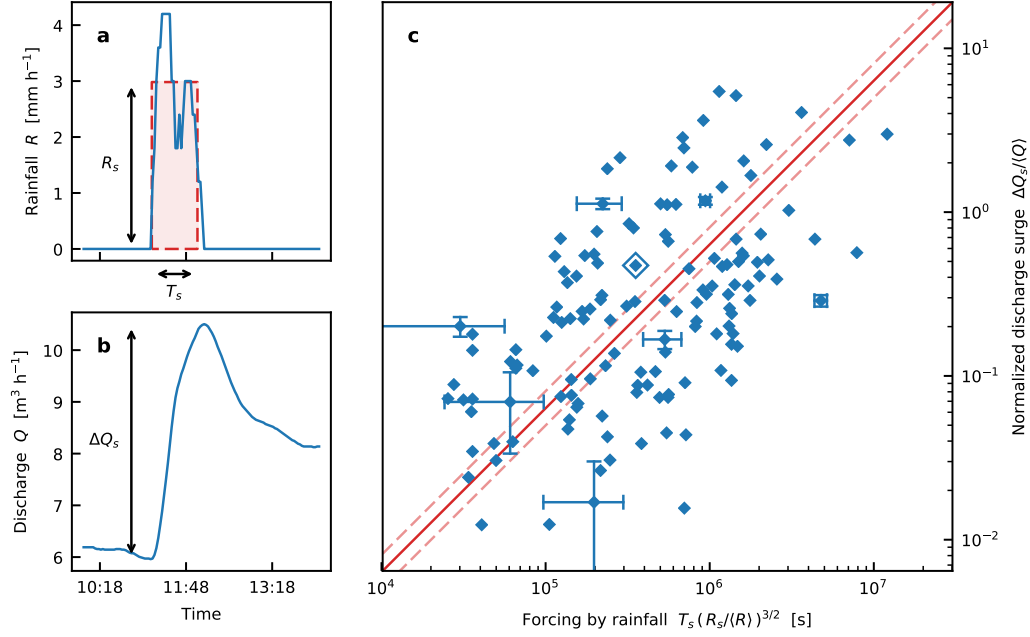


Figure 3. Relationship between rainfall intensity and associated surge in the stream discharge. (a) Rainfall event. Blue line shows actual time series superimposed over its mathematical representation (red dashed rectangle). The rectangle’s area, $R_s T_s$, and duration, T_s , are the integral and variance of the actual signal, respectively. (b) Surge of stream discharge caused by the rainfall event of panel A, with amplitude ΔQ_s . (c) Normalized discharge surge, $\Delta Q_s / \langle Q \rangle$, as a function of the product of the duration of the rainfall event, T_s , with the normalized rainfall intensity, $R_s / \langle R \rangle$, to the power 3/2 for 137 isolated rainfall events between January 2015 and October 2017. Error bars indicate measurement error (Supporting Information Text S3). Only a few error bars, selected for representativity, are shown. Rimmed marker indicates event of panels A and B. Solid red line shows proportionality (equation (5) with $T_c = 10.4$ days). Dashed red lines represent the standard deviation of T_c in logarithmic space.

257 We now compare the storm-flow regime with our field measurements. Let us consider
 258 a rainfall event such as the one of Figure 3a, which we idealize with a constant recharge rate
 259 R_s over a time T_s (Supporting Information Text S3). The aquifer responds to this input
 260 by delivering more water to the stream, the discharge of which thus surges (Figure 3b).
 261 Assuming that this surge is due mostly to the groundwater input, we can measure ΔQ_s
 262 on the hydrograph of the Quiock stream (Supporting Information Text S3), and normalize it
 263 with $\langle Q \rangle$, the average stream discharge. We now wish to compare this relative discharge
 264 surge to the storm-flow regime, embodied by Eq. (3). In doing so, we assume that the
 265 aquifer, or at least its shallower, most reactive part is virtually empty before the rainfall
 266 event. This, strictly speaking, is not true unless the stream dries out entirely. Still, this
 267 approximation can hold when the water table has enough time to recede between two rainfall
 268 events, but it is unlikely to hold when rains quickly follow each other.

269 Between January 2015 and October 2017, we have identified 137 isolated rainfall events,
 270 and measured the associated discharge surge ΔQ_s , rainfall intensity R_s , and total volume
 271 of water delivered to the catchment V_s (Supporting Information Text S3). Figure 3 shows
 272 these measurements in the coordinates suggested by equation (5), namely the normalized
 273 discharge surge $\Delta Q_s / \langle Q \rangle$, and the product of the rainfall duration, T_s , with the power 3/2

of the normalized rainfall intensity, $R_s/\langle R \rangle$, measured as shown on Figs. 3a and b. Both quantities spread over almost three orders of magnitude, revealing a positive correlation (the Pearson coefficient is 0.55 in logarithmic space), despite a significant scatter (about one order of magnitude). Fitting a power law to our data by orthogonal distance regression yields an exponent of 0.98 ± 0.09 , close to the exponent of one predicted by equation (5). Assuming this exponent is indeed one, we find that a characteristic time of $T_c \approx 10.4$ days best fits our data, which corresponds to an available volume of $V_a \approx 2400 \text{ m}^3$. We thus find that the fillable porosity is about $\phi_f \approx 1.3 \times 10^{-2}$, a value less than a fourth of the drainable porosity ϕ_d , as measured based on the recession flow—not a surprising observation (Acharya et al., 2012). These values however, should be treated with caution, as they inherit the uncertainty associated to the dispersion of the data in Figure 3 (at least a factor of 5).

Among the many hypotheses that allow one to derive equation (5), the existence (and location) of a horizontal impervious layer below the stream’s level is arguably the least substantiated. If, for comparison, we assume that such a layer lies a few meters below the stream’s level, the groundwater flow would not enter the storm-flow regime. Instead, we would expect it to enter the linear counterpart of this asymptotic behavior (provided the Boussinesq approximation still holds), and the stream’s discharge would then increase like $R_s\sqrt{T_s}$ (Pauwels & Troch, 2010; Pauwels & Uijlenhoet, 2019). Despite the scatter of Figure 3, there is little doubt that this linear regime does not fit our observations, thus supporting, in retrospect, the assumption of a fully-penetrating stream. Still, this simplifying hypotheses can only be a crude model of the Quiock aquifer, the actual geometry of which probably contributes to the dispersion of the data around the storm regime.

Often, the volume of groundwater that a catchment contains affects its response to the rainfall signal. This sensitivity to initial conditions could also explain part of the dispersion in Figure 3 (Biswal & Nagesh Kumar, 2014; Botter, Porporato, Rodriguez-Iturbe, & Rinaldo, 2009; Kirchner, 2009). Indeed, we may only expect the storm-flow regime to be a decent representation of the groundwater flow if the aquifer is essentially empty before the rainfall event. (Even in the framework of the Boussinesq approximation, the initial shape of the water table influences the response of the groundwater flow to recharge.) To evaluate the state of the groundwater flow before a rainfall event, we measure the discharge Q_i of the stream just before it rises, for the 137 events of Figure 3 (Supporting Information Text S8). Surprisingly, once detrended according to equation (5), the response of the stream’s discharge appears uncorrelated with the ratio $Q_i/\Delta Q_s$, even when the latter becomes larger than one—that is, when we would expect the storm-flow regime to break down (Supporting Information Figure S4a). A different picture emerges if we normalize the initial discharge with the average discharge of the stream ($Q_i/\langle Q \rangle$) then becomes our proxy for the groundwater’s state, Supporting Information Figure S4b). The prefactor of equation (5) increases significantly with this ratio, showing the influence of initial conditions on the groundwater’s response to rainfall events, but this correlation disappears for the most isolated events ($Q_i/\langle Q \rangle$ less than about 0.1). Repeating this analysis with the elevation of the water table in piezometer G confirms these observations, although with a lesser statistical significance (Supporting Information Figure S4c and S4d).

It is remarkable that the power-law relation associated to the storm-flow regime appears to hold even for rainfall events that are not, strictly speaking, isolated from the previous ones—although such events probably cause some of the scatter visible in Figure 3. If we restrict the analysis to the most isolated rainfall events, thus reducing our data set to only ten points, we find that a critical time of $T_c \approx 49$ days best fits our observations (Supporting Information Text S8). Although less significant statistically, this value might be more relevant physically. If so, the available volume of water in the catchment would be closer to $V_a \approx 11000 \text{ m}^3$, and the associated fillable porosity would be $\phi_f \approx 6.0 \times 10^{-2}$ —very close to the drainable porosity.

5 Conclusion

Like most field observations, our measurements are highly variable, and the Boussinesq approximation can only provide a rudimentary model of the groundwater dynamics during a rainfall event. Even where this approximation is appropriate, we can only expect the storm-flow regime to occur during rainfall events that are isolated from previous ones. Nonetheless, this regime expresses itself unambiguously in the hydrograph of the Quioc Creek, thus displaying the typical robustness of asymptotic regimes (Barenblatt, 1996). Among the rainfall events we have identified over 3 years, only a few qualify as floods—none of them catastrophic. The trend shown on Fig. 3c, however, shows no sign of abating, and the scaling law of the storm-flow regime might fit more severe events than those of our data set.

We suggest that the storm-flow regime takes place in many catchments where groundwater flows through a shallow unconfined aquifer. It would thus contribute to the widespread non-linearity of small catchments (Botter et al., 2009; Buttle, Dillon, & Eerkes, 2004; Kirchner, 2009; Tromp-van Meerveld & McDonnell, 2006; Uchida, Tromp-van Meerveld, & McDonnell, 2005). Of course, we would need more high-frequency rainfall and discharge measurements to support this hypothesis. Provided such time series, the plot of Figure 3 makes it straightforward to calibrate equation (5), which in turn can be implemented either as a source term in watershed models (Thompson, Sørensen, Gavin, & Refsgaard, 2004), or included in low-dimensional, physically-based models of the groundwater dynamics (Basso, Schirmer, & Botter, 2016; Kirchner, 2009). We trust this could improve flood forecasting in catchments dominated by shallow groundwater. In addition, the calibration of equation (5) yields the average volume of groundwater, V_a , that a catchment stores above the stream level—an estimate of the amount of water that will be released during a prolonged drought.

Finally, as a solution of the non-linear Boussinesq equation, the storm-flow regime reconciles the classical drought flow with the quick response of groundwater to rainfall. This encouraging finding bolsters the renewed interest in Boussinesq’s theory that high-frequency measurement devices have fostered (Troch et al., 2013).

Acknowledgments

All the time series used in this paper were collected by the *Observatoire de l’eau et de l’érosion aux Antilles* (ObsERA, INSU-CNRS). They are available at <http://webobsera.ipgp.fr/>. We thank the members of the *Observatoire Volcanologique et Sismologique de Guadeloupe*, and specially O. Crispi, for technical support. We are grateful to the *Parc National de la Guadeloupe*, and specially to S. La Pierre de Melinville and M. Gombauld, for granting us access to the field site. We thank S. Basso for suggesting, during the review process, to introduce the characteristic time of equation (5).

References

- Abdul, A., & Gillham, R. (1984). Laboratory studies of the effects of the capillary fringe on streamflow generation. *Water Resources Research*, *20*(6), 691–698.
- Abdul, A., & Gillham, R. (1989). Field studies of the effects of the capillary fringe on streamflow generation. *Journal of Hydrology*, *112*(1-2), 1–18.
- Acharya, S., Jawitz, J. W., & Mylavarapu, R. S. (2012). Analytical expressions for drainable and fillable porosity of phreatic aquifers under vertical fluxes from evapotranspiration and recharge. *Water Resources Research*, *48*(11).
- Barenblatt, G. I. (1996). *Scaling, self-similarity, and intermediate asymptotics: dimensional analysis and intermediate asymptotics* (Vol. 14). Cambridge University Press.
- Basso, S., Schirmer, M., & Botter, G. (2016). A physically based analytical model of flood frequency curves. *Geophysical Research Letters*, *43*(17), 9070–9076.
- Batu, V. (1998). *Aquifer hydraulics: a comprehensive guide to hydrogeologic data analysis* (Vol. 1). John Wiley & Sons.

- 374 Berkowitz, B. (2002). Characterizing flow and transport in fractured geological media: A
 375 review. *Advances in water resources*, *25*(8), 861–884.
- 376 Beven, K. (1981). Kinematic subsurface stormflow. *Water Resources Research*, *17*(5),
 377 1419-1424.
- 378 Beven, K., & Germann, P. (1982). Macropores and water flow in soils. *Water resources*
 379 *research*, *18*(5), 1311-1325.
- 380 Biswal, B., & Nagesh Kumar, D. (2014). Study of dynamic behaviour of recession curves.
 381 *Hydrological Processes*, *28*(3), 784–792.
- 382 Botter, G., Porporato, A., Rodriguez-Iturbe, I., & Rinaldo, A. (2009). Nonlinear storage-
 383 discharge relations and catchment streamflow regimes. *Water resources research*,
 384 *45*(10).
- 385 Boussinesq, J. (1904). Recherches théoriques sur l'écoulement des nappes d'eau infiltrées
 386 dans le sol et sur le débit des sources. *Journal de mathématiques pures et appliquées*,
 387 *5*-78.
- 388 Brutsaert, W., & Nieber, J. L. (1977). Regionalized drought flow hydrographs from a
 389 mature glaciated plateau. *Water Resources Research*, *13*(3), 637-643.
- 390 Buss, H. L., White, A. F., Dessert, C., Gaillardet, J., Blum, A. E., & Sak, P. B. (2010).
 391 Depth profiles in a tropical volcanic critical zone observatory: Basse-terre, guadeloupe.
 392 In *Proc. of the 13th intl. symp. on water-rock interaction*.
- 393 Buttle, J. M., Dillon, P. J., & Eerkes, G. R. (2004, feb). Hydrologic coupling of slopes, ri-
 394 parian zones and streams: an example from the canadian shield. *Journal of Hydrology*,
 395 *287*(1), 161-177. doi: 10.1016/j.jhydrol.2003.09.022
- 396 Cardenas, M. B. (2007). Potential contribution of topography-driven regional groundwater
 397 flow to fractal stream chemistry: Residence time distribution analysis of toth flow.
 398 *Geophysical Research Letters*, *34*(5).
- 399 Clergue, C., Dellinger, M., Buss, H. L., Gaillardet, J., Benedetti, M. F., & Dessert, C.
 400 (2015). Influence of atmospheric deposits and secondary minerals on li isotopes budget
 401 in a highly weathered catchment, guadeloupe (lesser antilles). *Chemical Geology*, *414*,
 402 28-41. doi: 016/j.chemgeo.2015.08.015
- 403 Cloke, H., Anderson, M., McDonnell, J., & Renaud, J.-P. (2006). Using numerical mod-
 404 elling to evaluate the capillary fringe groundwater ridging hypothesis of streamflow
 405 generation. *Journal of Hydrology*, *316*(1-4), 141–162.
- 406 Colmet-Daage, F., & Lagache, P. (1965). Caractéristiques de quelques groupes de sols
 407 dérivés de roches volcaniques aux antilles françaises. *Cahiers de l'ORSTOM serie*
 408 *pédologie*, *8*, 91-121.
- 409 De Marsily, G., Delay, F., Goncalves, J., Renard, P., Teles, V., & Violette, S. (2005). Dealing
 410 with spatial heterogeneity. *Hydrogeology Journal*, *13*(1), 161–183.
- 411 Dupuit, J. (1848). *Etudes theoriques et pratiques sur le mouvement des eaux courantes*.
 412 Carilian-Goeury.
- 413 Fiori, A. (2012). Old water contribution to streamflow: Insight from a linear boussinesq
 414 model. *Water Resources Research*, *48*(6).
- 415 Fiori, A., Romanelli, M., Cavalli, D., & Russo, D. (2007). Numerical experiments of
 416 streamflow generation in steep catchments. *Journal of hydrology*, *339*(3-4), 183–192.
- 417 Goderniaux, P., Davy, P., Bresciani, E., Dreuzy, J.-R., & Le Borgne, T. (2013). Parti-
 418 tioning a regional groundwater flow system into shallow local and deep regional flow
 419 compartments. *Water Resources Research*, *49*(4), 2274–2286.
- 420 Guérin, A., Devauchelle, O., & Lajeunesse, E. (2014, nov). Response of a laboratory aquifer
 421 to rainfall. *Journal of Fluid Mechanics*, *759*, -1. doi: 10.1017/jfm.2014.590
- 422 Harman, C., & Sivapalan, M. (2009). A similarity framework to assess controls on shal-
 423 low subsurface flow dynamics in hillslopes. *Water Resources Research*, *45*(1), n/a–
 424 n/a. Retrieved from <http://dx.doi.org/10.1029/2008WR007067> (W01417) doi:
 425 10.1029/2008WR007067
- 426 Jasechko, S., Kirchner, J. W., Welker, J. M., & McDonnell, J. J. (2016, feb). Substantial
 427 proportion of global streamflow less than three months old. *Nature Geoscience*, *9*,
 428 126-129. doi: 10.1038/NGEO2636

- 429 Kirchner, J. W. (2003). A double paradox in catchment hydrology and geochemistry.
430 *Hydrological Processes*, *17*(4), 871-874. doi: 10.1002/hyp.5108
- 431 Kirchner, J. W. (2009). Catchments as simple dynamical systems: Catchment characteri-
432 zation, rainfall-runoff modeling, and doing hydrology backward. *Water Resources Re-*
433 *search*, *45*(2), n/a–n/a. Retrieved from <http://dx.doi.org/10.1029/2008WR006912>
434 (W02429) doi: 10.1029/2008WR006912
- 435 Maher, K., DePaolo, D. J., Conrad, M. E., & Serne, R. J. (2003). Vadose zone infiltration
436 rate at hanford, washington, inferred from sr isotope measurements. *Water Resources*
437 *Research*, *39*(8).
- 438 Mares, R., Barnard, H. R., Mao, D., Revil, A., & Singha, K. (2016). Examining diel patterns
439 of soil and xylem moisture using electrical resistivity imaging. *Journal of Hydrology*,
440 *536*, 327–338.
- 441 McDonnell, J. J. (1990). A rationale for old water discharge through macropores in a steep,
442 humid catchment. *Water Resources Research*, *26*(11), 2821-2832.
- 443 McDonnell, J. J. (2003, jun). Where does water go when it rains?: Moving beyond the
444 variable source area concept of rainfall-runoff response. *Hydrological processes*, *17*(9),
445 1869-1875. doi: 10.1002/hyp.5132
- 446 McDonnell, J. J., McGuire, K., Aggarwal, P., Beven, K. J., Biondi, D., Destouni, G.,
447 ... others (2010). How old is streamwater? open questions in catchment transit time
448 conceptualization, modelling and analysis. *Hydrological Processes*, *24*(12), 1745–1754.
- 449 McGlynn, B. L., McDonnell, J. J., & Brammer, D. D. (2002). A review of the evolving per-
450 ceptual model of hillslope flowpaths at the maimai catchments, new zealand. *Journal*
451 *of Hydrology*, *257*(1-4), 1–26.
- 452 McKay, L. D., Driese, S. G., Smith, K. H., & Vepraskas, M. J. (2005). Hydrogeology and
453 pedology of saprolite formed from sedimentary rock, eastern tennessee, usa. *Geoderma*,
454 *126*(1-2), 27–45.
- 455 Montgomery, D. R., Dietrich, W. E., Torres, R., Anderson, S. P., Heffner, J. T., & Loague,
456 K. (1997). Hydrologic response of a steep, unchanneled valley to natural and applied
457 rainfall. *Water Resources Research*, *33*(1), 91–109.
- 458 Neal, C., & Rosier, P. T. (1990). Chemical studies of chloride and stable oxygen isotopes in
459 two conifer afforested and moorland sites in the british uplands. *Journal of Hydrology*,
460 *115*(1-4), 269–283.
- 461 Park, E., & Parker, J. (2008). A simple model for water table fluctuations in response to
462 precipitation. *Journal of Hydrology*, *356*(3-4), 344–349.
- 463 Pauwels, V. R. N., & Troch, P. A. (2010). Estimation of aquifer lower layer hydraulic
464 conductivity values through base flow hydrograph rising limb analysis. *Water resources*
465 *research*, *46*(3). doi: 10.1029/2009WR008255
- 466 Pauwels, V. R. N., & Uijlenhoet, R. (2019). Confirmation of a short-time expression
467 for the hydrograph rising limb of an initially dry aquifer using laboratory hillslope
468 outflow experiments. *Water Resources Research*, *0*(0). Retrieved from [https://](https://agupubs.onlinelibrary.wiley.com/doi/abs/10.1029/2018WR023580)
469 agupubs.onlinelibrary.wiley.com/doi/abs/10.1029/2018WR023580 doi: 10
470 .1029/2018WR023580
- 471 Rupp, D. E., Schmidt, J., Woods, R. A., & Bidwell, V. J. (2009). Analytical assessment and
472 parameter estimation of a low-dimensional groundwater model. *Journal of hydrology*,
473 *377*(1-2), 143–154.
- 474 Sanchez-Vila, X., Guadagnini, A., & Carrera, J. (2006). Representative hydraulic conduc-
475 tivities in saturated groundwater flow. *Reviews of Geophysics*, *44*(3).
- 476 Schoeneberger, P., & Amoozegar, A. (1990). Directional saturated hydraulic conductivity
477 and macropore morphology of a soil-saprolite sequence. *Geoderma*, *46*(1-3), 31–49.
- 478 Sefton, C., Whitehead, P., Eatherall, A., Littlewood, I., & Jakeman, A. (1995). Dynamic
479 response characteristics of the plynlimon catchments and preliminary analysis of rela-
480 tionships to physical descriptors. *Environmetrics*, *6*(5), 465–472.
- 481 Sidle, R. C., Tsuboyama, Y., Noguchi, S., Hosoda, I., Fujieda, M., & Shimizu, T.
482 (2000). Stormflow generation in steep forested headwaters: a linked hydrogeomor-
483 phic paradigm. *Hydrological Processes*, *14*(3), 369-385.

- 484 Sklash, M. (1990). Environmental isotope studies of storm and snowmelt runoff generation.
485 *Process studies in hillslope hydrology*, 401–436.
- 486 Sklash, M. G., & Farvolden, R. N. (1979). The role of groundwater in storm runoff.
487 *Developments in Water Science*, 12, 45–65.
- 488 Sophocleous, M. A. (1991). Combining the soilwater balance and water-level fluctuation
489 methods to estimate natural groundwater recharge: practical aspects. *Journal of*
490 *hydrology*, 124(3–4), 229–241.
- 491 Tani, M. (1997). Runoff generation processes estimated from hydrological observations on
492 a steep forested hillslope with a thin soil layer. *Journal of Hydrology*, 200(1), 84–109.
- 493 Thompson, J., Sørensen, H. R., Gavin, H., & Refsgaard, A. (2004). Application of the
494 coupled mike she/mike 11 modelling system to a lowland wet grassland in southeast
495 england. *Journal of Hydrology*, 293(1), 151–179.
- 496 Toth, J. (1963). A theoretical analysis of groundwater flow in small drainage basins. *Journal*
497 *of geophysical research*, 68(16), 4795–4812.
- 498 Troch, P. A., Berne, A., Bogaart, P., Harman, C., Hilberts, A. G., Lyon, S. W., ... others
499 (2013). The importance of hydraulic groundwater theory in catchment hydrology: The
500 legacy of wilfried brutsaert and jean-yves parlange. *Water Resources Research*, 49(9),
501 5099–5116.
- 502 Tromp-van Meerveld, H., & McDonnell, J. (2006). Threshold relations in subsurface storm-
503 flow: 2. the fill and spill hypothesis. *Water Resources Research*, 42(2).
- 504 Uchida, T., Tromp-van Meerveld, I., & McDonnell, J. J. (2005, sep). The role of lateral pipe
505 flow in hillslope runoff response: an intercomparison of non-linear hillslope response.
506 *Journal of Hydrology*, 311(1), 117–133. doi: 10.1016/j.jhydrol.2005.01.012